Clim. Past, 20, 335–348, 2024
https://doi.org/10.5194/cp-20-335-2024

Climate of the Past
Open Access
EGU

BrGDGT-based seasonal paleotemperature reconstruction for the last 15 000 years from a shallow lake on the eastern Tibetan Plateau

Xiaohuan Hou[1], Nannan Wang[1], Zhe Sun[2], Kan Yuan[1,3], Xianyong Cao[1], and Juzhi Hou[1]

[1]Group of Alpine Paleoecology and Human Adaptation (ALPHA), State Key Laboratory of Tibetan Plateau Earth System, Resources and Environment (TPESRE), Institute of Tibetan Plateau Research, Chinese Academy of Sciences, Beijing 100101, China
[2]Institute of Geography and Resources Science, Sichuan Normal University, Chengdu, 610066, China
[3]College of Resources and Environment, University of Chinese Academy of Sciences, Beijing, 100049, China

Correspondence: Juzhi Hou (houjz@itpcas.ac.cn)

Received: 14 May 2023 – Discussion started: 24 May 2023
Revised: 19 December 2023 – Accepted: 20 December 2023 – Published: 13 February 2024

Abstract. Understanding Holocene temperature changes is vital for resolving discrepancies between proxy reconstructions and climate models. The intricate temperature variations across the Tibetan Plateau (TP) add complexity to studying continental climate change during this period. Discrepancies between model-based and proxy-based reconstructions might stem from seasonal biases and environmental uncertainties in the proxies. Employing multiple proxies from a single sediment core for quantitative temperature reconstructions offers an effective method for cross-validation in terrestrial environments. Here, we present an ice-free-season temperature record for the past 15 kyr from a shallow, freshwater lake on the eastern TP, based on brGDGTs (branched glycerol dialkyl glycerol tetraethers). This record shows that the Holocene Thermal Maximum lags the pollen-based July temperature recorded in the same sediment core. We conclude that the mismatch between the brGDGT-based and pollen-based temperatures is primarily the result of seasonal variations in solar irradiance. The overall pattern of temperature changes is supported by other summer temperature records, and the Younger Dryas cold event and the Bølling–Allerød warm period are also detected. A generally warm period occurred during 8–3.5 ka, followed by a cooling trend in the late Holocene. Our findings have implications for understanding the seasonal signal of brGDGTs in shallow lakes and provide critical data for confirming the occurrence of seasonal biases in different proxies from high-elevation lakes. To further investigate the significance of the brGDGTs and temperature patterns on the TP, we examined existing brGDGT-based Holocene temperature records, which interpret these compounds as indicators of mean annual or growing season temperatures. The existing and available temperature records show complicated patterns of variation, some with general warming trends throughout the Holocene, some with cooling trends, and some with a warm middle Holocene. We analyzed the possible reasons for the diverse brGDGTs records on the TP and emphasize the importance of considering lake conditions and modern investigations of brGDGTs in lacustrine systems when using brGDGTs to reconstruct paleoenvironmental conditions.

1 Introduction

Global climate change has a profound impact on both the natural ecological and socio-economic systems that are vital for human survival and development, making climate change a critical limiting factor for the sustainable development of human society. The Tibetan Plateau (TP), also called the "Third Pole" (Qiu, 2008), has undergone a more rapid warming over the last 5 decades, with a rate twice that of the global average (0.3–0.4 °C per decade) (Kuang and Jiao, 2016; Chen et al., 2015), making it one of the world's most temperature-sensitive regions (Chen et al., 2015; Yao et al., 2022). Consequently, assessing the impact of future climate change on

the TP is becoming increasingly important. To enhance the precision and accuracy of future climate change estimates for the TP under ongoing global climate change and to minimize the uncertainty in climate simulations, it is essential to investigate the processes and mechanisms of regional climate and environmental changes, with particular emphasis on temperature, on a relatively long timescale, such as that of the Holocene.

The Holocene, the most recent geological epoch, is closely linked with the development of human civilization. Quantitative reconstructions of Holocene temperature trends can be used to explore their impacts on civilization and to establish a geological and historical context for predicting future climate changes. In recent decades, many Holocene quantitative reconstructions of seasonal and annual temperatures for the TP have been produced using various proxies, like pollen (Herzschuh et al., 2014; Lu et al., 2011), chironomids (E. Zhang et al., 2017, 2019), $\delta^{18}O$ in ice cores (Pang et al., 2020; Thompson et al., 1997), and biomarkers (Hou et al., 2016; Zhao et al., 2013; Cheung et al., 2017). These reconstructions have provided crucial data for the elucidation of Holocene temperature changes. However, the available Holocene temperature records from the TP show divergent trends. Multiple proxy indicators indicate three different Holocene temperature patterns on the TP. First, a consistent Holocene warming trend (Sun et al., 2022; Feng et al., 2022; Opitz et al., 2015). For example, annual temperatures based on brGDGTs (branched glycerol dialkyl glycerol tetraethers; Feng et al., 2022; Sun et al., 2022) indicate a gradual warming trend that resembles the $\delta^{18}O$ temperature record from the Chongce ice core on the western TP, except for the last 2 ka (Pang et al., 2020). Second, an early to middle Holocene summer temperature maximum and a gradual cooling trend during the late Holocene are observed in pollen-, alkenone-, and chironomid-based temperature records (Herzschuh et al., 2014; Hou et al., 2016; Zhang et al., 2017; G. Wang et al., 2021; Zheng et al., 2015). Third, a prominent relatively cool middle Holocene (M. Wang et al., 2021; Li et al., 2017); for example, a composite temperature record suggests that temperatures were $\sim 2\,^{\circ}C$ cooler during the middle Holocene than during the early and late Holocene (M. Wang et al., 2021). Several records also show a steady long-term trend without distinct cooling or warming (Sun et al., 2021). Moreover, the cooling trends in proxy-based Holocene temperature records are inconsistent with those of climate models, which indicate a warming trend, and this inconsistency is widely known as the "Holocene temperature conundrum" (Liu et al., 2014). There are several potential factors that may contribute to the disparity in Holocene temperature trends, including seasonal biases and uncertainties in temperature proxies and reconstructions, independent of climate models (Liu et al., 2014; Hou et al., 2019; Bova et al., 2021; Cartapanis et al., 2022; Marsicek et al., 2018). While several recent studies have suggested that seasonality in proxies is not the major cause of the Holocene temperature conundrum (Dong et al., 2022; W. Zhang et al., 2022), it is significant that the TP is an alpine and high-altitude region with significant seasonal temperature variations. Moreover, most organisms tend to grow during the warmer seasons at high latitudes and high altitudes (B. Zhao et al., 2021). Currently, however, we lack unambiguous and reliable seasonal temperature records to support a seasonality bias hypothesis. Extensive research has been conducted in lakes, employing a single proxy to reconstruct past temperature fluctuations. However, there have been scarce studies that employ various proxies within the same core to reconstruct paleotemperature variations. Furthermore, the limited number of studies primarily concentrate on reconstructing summer temperature and annual average temperature. For example, a chironomid-based July temperature reconstruction for Tiancai lake on the southeastern TP shows higher temperatures during the early to middle Holocene (Zhang et al., 2017), while the brGDGT-based annual average temperature shows a warming trend (Feng et al., 2022). Different proxies may reflect the seasonal temperatures in different months, and thus producing temperature reconstructions for different months for the same sediment core may help us to better understand the seasonal bias of terrestrial temperature records. Furthermore, the reconciliation of the divergent trends of Holocene temperature on the TP and its surroundings requires additional high-altitude temperature records from these regions, with reliable chronologies and proxy records with an unambiguous climatological significance.

BrGDGTs are a group of membrane-spanning lipids found in bacteria (Fig. S1) (Chen et al., 2022; Halamka et al., 2022; Sinninghe Damsté et al., 2000), and they have become a powerful tool for quantifying past terrestrial temperature variations. Through investigations of brGDGTs in globally distributed soils, it was found that the distribution of brGDGTs is primarily related to temperature and pH (Weijers et al., 2007). Subsequently, brGDGT–temperature calibrations from soil, peat, and lake sediments were established on scales from global (Weijers et al., 2007; De Jonge et al., 2014; Crampton-Flood et al., 2020; Martínez-Sosa et al., 2021) to regional (e.g., East Asia) (Sun et al., 2011; Ding et al., 2015; Wang et al., 2016; Dang et al., 2018), leading to considerable progress in reconstructing terrestrial temperatures, particularly on the TP (Cheung et al., 2017; C. Zhang et al., 2022; Li et al., 2017).

Natural lakes are widely distributed across the TP (G. Zhang et al., 2019). Lake sediments, characterized by their organic matter-rich composition, exhibit continuous and rapid accumulation rates. As a result, they offer high-resolution records of environmental changes, making them highly valued as a primary terrestrial climate archive (Moser et al., 2019). BrGDGTs in lacustrine systems are often more strongly correlated with temperature, with higher coefficient of determination (r^2) and lower root-mean-square error (RMSE) values (Martínez-Sosa et al., 2021) than in soils and peats. Nevertheless, the factors that impact the distribution

of brGDGTs in lakes are intricate and multidimensional. Notably, the sources of brGDGTs within lakes are intricate, involving contributions from soil as well as autochthonous lake processes. However, an expanding body of research underscores a substantial prevalence of autochthonous brGDGTs in lakes (Tierney and Russell, 2009; Tierney et al., 2010; Weber et al., 2015; H. Wang et al., 2021). Furthermore, the origins of brGDGT producers remain uncertain and could be influenced by various factors, including lake salinity (H. Wang et al., 2021), redox conditions (Weber et al., 2018), oxygen content and/or mixing patterns (Van Bree et al., 2020; Wu et al., 2021; Buckles et al., 2014). Additionally, even lake depth plays a role due to distinct ecological niches (Woltering et al., 2012), thereby contributing to the intricate interplay that shapes the distribution of brGDGTs within lakes.

In this study, we obtained a quantitative temperature reconstruction for the past 15 ka from Gahai, a shallow (average depth of ~ 2 m) freshwater lake located in the source area of the Yellow River. This region is an important ecological protection area on the eastern edge of the TP. Freshwater environments avoid the confounding effects of salinity on brGDGT-based temperature reconstructions, and shallow lakes also minimize the impact of the uneven distribution of light and nutrients on brGDGTs. Our specific aims were (1) to determine the long-term trend of Holocene warm-biased terrestrial temperatures at a high elevation; (2) to compare records of ice-free season temperatures with July temperatures from the same sediment core; and (3) to gain a better understanding of the possible mechanisms responsible for Holocene temperature variations, especially on the TP.

2 Materials and methods

2.1 Study site

Gahai (34°04′–34°4′ N, 102°11′–102°28′ E, 3444 m a.s.l.) is a freshwater lake and part of the Gahai meadow wetland, which is a national nature reserve with restricted human access on the eastern edge of the TP (Fig. 1). The lake is fed by runoff from the surrounding hills, drains into the Tao River, and ultimately enters the Yellow River. Thus, Gahai lake is a critical water conservation area in the upper reaches of the Yellow River. The average water depth of Gahai is ~ 2 m, and the maximum depth is ~ 5 m. The vegetation in the catchment consists mainly of *Kobresia tibetica, Equisetum arvense, Potentilla anserina, Artemisia subulate*, and *Oxytropis falcata* (Ma et al., 2019). Meteorological data for the area are available from Langmu Temple station (1957–1988) (Fig. 1) (34°5′ N, 102°38′ E, 3412 m a.s.l.), ~ 32 km northwest of Gahai lake. They indicate an annual average (mean) precipitation of 781 mm, with >67 % occurring between June and September, and mean annual temperature of 1.2 °C with a relative humidity of ~ 65 %. The summers are mild and humid, and the winters are cold and dry. From May to September, the mean average temperature is above freezing (0 °C), but the temperature in May is very low, close to 0 °C.

2.2 Sampling

A sediment core with a length of 329 cm was obtained from Gahai lake in January 2019 at a water depth of 1.95 m using a UWITEC platform operated from the frozen lake surface. In addition, four catchment soil samples were collected from around the lake (Fig. 1). All samples were transported to the Institute of Tibetan Plateau Research, Chinese Academy of Sciences (ITPCAS). The sediment core was split lengthwise, and one half was subsampled and freeze-dried for subsequent analysis.

2.3 Chronology

The chronology of the upper 20 cm of the sediment core is based on measurements of ^{210}Pb and ^{137}Cs, at a 1 cm interval. The chronology for the deeper part of the core is provided by accelerator mass spectrometry (AMS) ^{14}C measurements of 13 bulk sediment samples, which were conducted by Beta Analytic Inc. (Miami, USA) (Fig. 2) (Wang et al., 2022).

The ^{210}Pb age model was constructed using the constant rate of supply (CRS) model and the ^{137}Cs peak was used as a supplement (Appleby, 2002). The calculated age of ^{210}Pb using CRS model aligned well with the ^{137}Cs peak at 6 cm. Overall, the CRS model was deemed suitable for determining the age of Gahai lake.

Reservoir age, as highlighted by Hou et al. (2012), is a crucial factor affecting the age determination of lake sediment cores on the TP. Therefore, it was necessary to establish the reservoir age of Gahai lake before undertaking paleoclimate reconstruction. The linear extrapolation relationship between the ^{14}C ages and depth to the sediment–water interface is often used to estimate the reservoir age. The ^{14}C age of 13 samples exhibits a good linear relationship with sediment depth in Gahai lake. Extrapolation of the 13 total ^{14}C ages down to the depth of 6 cm yielded a ^{14}C age of 461 yr BP, while the reliable ^{210}Pb age at 6 cm is -27 yr BP. Consequently, the difference between the two ages, which amounts to 488 years, was taken as the reservoir age. Additionally, it is worth noting that independent estimations of the ^{14}C calibration age and ^{210}Pb age around 10 cm in Gahai lake were obtained, resulting in values of 497 and 18 yr BP, respectively. The difference of 479 years between these two ages can also be considered the reservoir age. These two methods of estimating reservoir age of Gahai lake show very close results that are mutually supportive. So, the average of 483 years was adopted as the reservoir age. All original ^{14}C dates were corrected by subtracting the reservoir age (483 years) and calibrating them to calendar ages using Calib 8.1. The age–depth model (Fig. 2) was constructed using the Bacon program with the ^{14}C ages

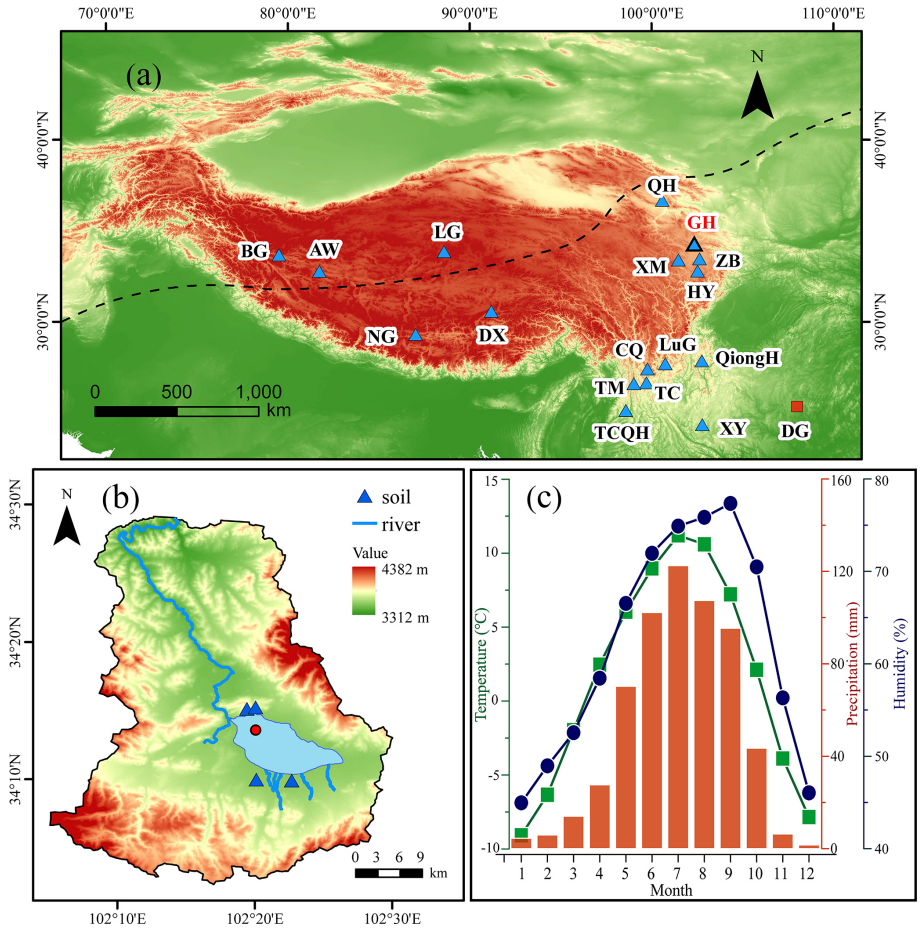

Figure 1. **(a)** Locations of the sites on the Tibetan Plateau referenced in the text. Triangle with bold line indicates the location of Gahai lake (this study). Other triangles indicate the locations of cited studies on the TP and the surrounding area: Bangong Co (BG), Aweng Co (AW), Ngamring Co (NG), Linggo Co (LG), Dangxiong wetland (DX), Qinghai lake (QH), Ximen Co (XM), Zoige basin (ZB), Hongyuan peatland (HY), Lugu lake (LuG), Cuoqia lake (CQ), Tingming lake (TM), Tengchongqinghai lake (TCQH), Tiancai lake (TC), Qionghai lake (QH), and Xingyun lake (XY). The red square indicates Dongge Cave (DG). The dotted black line represents the northern boundary of the modern Asian summer Monsoon (Chen et al., 2008). **(b)** Drainage basin of Gahai lake and the core site. **(c)** Climate data from Langmu Temple meteorological station: monthly temperature (green line), precipitation (red bars), and humidity (navy blue line).

and ^{210}Pb ages (Blaauw and Andres Christen, 2011) and was reported by Wang et al. (2022).

2.4 Lipids extraction and brGDGTs analysis

For lipids extraction, ~ 5 g samples were ground to a powder and extracted ultrasonically with dichloromethane (DCM) : methanol(MeOH) (9 : 1, v : v) three times. The supernatants were combined and dried under a stream of nitrogen gas. Subsequently, the total lipid extracts were separated into neutral and acid fractions through a LC-NH_2 silica gel column using DCM : isopropylalcohol (2 : 1, v : v) and ether with 4 % acetic acid (v : v), respectively. The neutral fraction was then eluted through a silica gel column using *n*-hexane, DCM, and MeOH, and the GDGTs were dissolved in the MeOH. The GDGTs fraction was passed through a 0.45 µm polytetrafluoroethylene (PTFE) filter before analysis. C_{46}-GDGT (a standard compound) (Huguet et al., 2006) was added to the samples before analysis.

BrGDGTs were detected using a high-performance liquid chromatography–atmospheric pressure chemical ionization–mass spectrometry (HPLC-APCI-MS) (Waters ACQUITY UPLC I-Class/Xevo TQD) with auto-injection at the ITP-CAS. The compounds were separated by three Hypersil Gold Silica LC columns in sequence (each 100 mm × 2.1 mm, 1.9 µm, Thermo Fisher Scientific; USA) and maintained at a temperature of 40 °C. GDGTs were eluted isocratically using 84 % hexane and 16 % ethyl acetate (EtOA) for the first 5 min, followed by a linear gradient change to 82 % hexane and 18 % EtOA from 5 to 65 min. The columns were cleaned using 100 % EtOA for 10 min and then back to 84 % hexane and 16 % EtOA to equilibrate the column, with a flow rate of 0.2 mL min^{-1}.

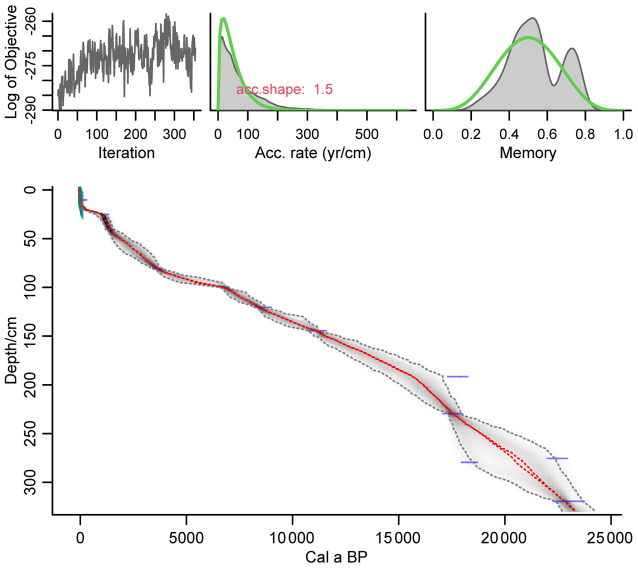

Figure 2. Age–depth model for Gahai, based on AMS ^{14}C, ^{210}Pb, and ^{137}Cs ages (Wang et al., 2022). The ages of the upper 20 cm are based on ^{210}Pb and ^{137}Cs dating (green symbols) and those of the lower part on AMS ^{14}C dates (blue symbols).

The APCI-MS conditions were as follows: nebulizer pressure at 60 psi, APCI probe temperature at 400 °C, drying gas flow rate of 6 L min^{-1} and temperature of 200 °C, capillary voltage of 3600 V, and source corona of 5.5 µA. Detection was performed in selected ion monitoring (SIM) mode, targeting the protonated molecules at m/z for the GDGTs, such as 1050, 1048, 1046, 1036, 1034, 1032, 1022, 1020, 1018, and 744. The results were analyzed using MassLynx V4.1 software, and quantification was achieved by comparing the peak areas of targeted ions and the internal standard, assuming an identical response factor for GDGTs.

3 Results and discussion

3.1 Concentration and distribution of brGDGTs in the sediment core and catchment soils

BrGDGTs were detected in both the catchment soils and the downcore sediments. The average concentration of brGDGTs in the catchment soils (0.07 ng g^{-1} dw, dry weight) was lower than in the surficial core sediments (0.70 ng g^{-1} dw). In the soil samples, pentamethylated brGDGTs were generally the most abundant (55.33 %), followed by tetramethylated brGDGTs (23.60 %) and hexamethylated brGDGTs (21.07 %) (Fig. S2). The relative amount of cyclopentane ring-containing brGDGTs in the soil samples was generally low (24.34 %), and it was sometimes too low to be detected, especially the fractions of IIIb, IIIb', IIIc, IIIc', IIc, and IIc'. In the downcore sediments, the relative abundant of tetramethylated brGDGTs (43.84 %) was like that of pentamethylated brGDGTs (41.93 %), and hexamethylated brGDGTs were the least abundant (14.22 %) (Fig. S2). The relative abundant of cyclopentane ring-containing brGDGTs in the downcore sediments (67.82 %) was lower than that in the catchment soils.

3.2 In situ production of brGDGTs in Gahai lake

Although lacustrine brGDGTs have great potential for quantitatively reconstructing terrestrial paleotemperatures, uncertainties about their sources in lacustrine environments are a major factor limiting their application (Tierney and Russell, 2009; Cao et al., 2020; Sun et al., 2011; Sinninghe Damsté et al., 2009; Buckles et al., 2014). To investigate the origin and characteristics of brGDGTs in Gahai lake sediments, we examined the distributions and concentrations of brGDGTs in the sediments and catchment soils and found notable differences between them. First, as described in the previous section, the average content of brGDGTs in the catchment soils was ∼ 10 % that of the surficial lake sediments, suggesting the absence of large-scale allochthonous inputs from the catchment soils. Second, the brGDGTs distributions in the downcore sediments were quite different from those in the catchment soils, which suggests a substantial autochthonous brGDGTs contribution to the lake sediments (Figs. 3 and S2). Moreover, the ratios of 6-methyl brGDGTs to 5-methyl GDGTs (IR_{6ME}) in the soils and sediments, calculated according to the formula proposed by De Jonge et al. (2014), were different. In the soil samples, IR_{6ME} varied between 0.54 and 0.57 and the average ratio in the downcore samples was 0.26, varying between 0.18 and 0.47. Third, the in situ production of brGDGTs in Gahai lake is suggested by the discrepancies in the degree of methylation (MBT'_{5ME}) between the soils and surface sediments. The average value of MBT'_{5ME} in the Gahai lake surface sediments was 0.48, which is clearly higher than in the catchment soils, with the range of 0.32–0.35. Fourth, and potentially the most significant, the IIIb' and Ib' compounds are present in the catchments soil but not in the Gahai lake surficial sediments, which may be direct evidence of an autochthonous brGDGTs contribution in the lacustrine environment (Fig. 3) and a lower proportion of soil-derived brGDGTs input. Therefore, we conclude that the brGDGTs in the Gahai lake sediments are mainly of in situ origin.

3.3 The brGDGT temperature calibration and Holocene temperature reconstruction

Gahai is a shallow lake in the eastern TP that is typically completely frozen during winter and spring. Local meteorological data indicate that the average snowfall period lasts for 269 d, with around 50 d of continuous snowfall (Liang and Luo, 2006). The freezing of the lake surface begins in late October each year and gradually thaws starting from May of the following year. As a result, the light transmittance and oxygen content in the lake water are reduced during the

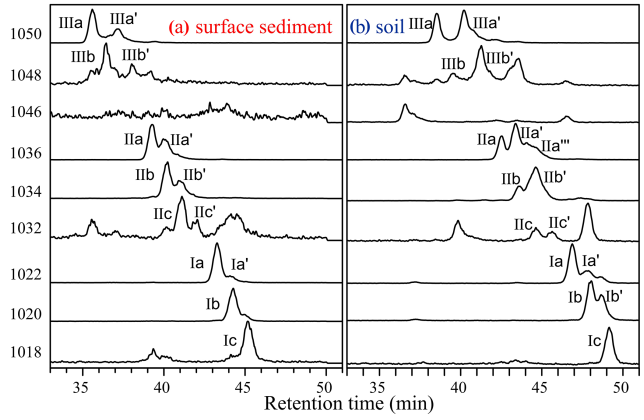

Figure 3. Representative high-performance liquid chromatography–atmospheric pressure chemical ionization–mass spectrometry (HPLC-APCI-MS) chromatograms of brGDGTs from **(a)** surface sediments from Gahai lake, and **(b)** soils in the catchment of Gahai lake.

freezing season, leading to decreased nutrient levels, which severely hinder the growth of autotrophic microorganisms. Although the bacteria responsible for producing brGDGTs have not been thoroughly characterized, the abundance of heterotrophic bacteria will likely decrease due to the reduced autotrophic biomass during the winter and spring ice-covered period. The weakened light penetration, decreased oxygen levels, and lack of nutrient replenishment during the frozen period significantly impact the growth of autochthonous microorganisms.

Furthermore, some research suggests that the production of brGDGTs might be related to factors such as water depth, seasonal alternation of water column mixing, and stratification (Loomis et al., 2014; Van Bree et al., 2020). During the summer and autumn seasons when the lake ice melts and the water becomes more mobile, the nutrient content increases, resulting in elevated lake biomass; moreover, the oxygen levels at the bottom of Gahai lake are not expected to be too high, which could further contribute to the proliferation of brGDGT-producing bacteria, potentially leading to an increase in the brGDGT-producing bacteria (Weber et al., 2018). Therefore, brGDGTs in Gahai lake may provide records of the average temperature during the ice-free months of the summer and autumn seasons.

Additionally, the presence of the frozen lake surface during winter creates a thermal barrier, impeding the exchange of heat between the lake water and the atmosphere. Consequently, any brGDGTs generated within the lake water during this period lose their ability to accurately reflect atmospheric temperature variations (Sun et al., 2021; C. Zhang et al., 2022). Thus, they were no longer able to track atmospheric temperature changes during the frozen season. Thus, we prefer to use Gahai brGDGTs to reconstruct temperatures during the summer and ice-free seasons. For this purpose, we employed the new Bayesian calibration for the mean temperature of the months above freezing (MAF), as proposed by Martínez-Sosa et al. (2021), to derive a MAF for Gahai lake.

To assess the accuracy of this calibration approach, we compared the fractional abundances of summed tetra-, penta-, and hexamethylated brGDGTs in Gahai lake sediments with other datasets (Fig. 4). These datasets include lake sediments from the TP (Günther et al., 2014; Wang et al., 2016), eastern Africa (Russell et al., 2018), and global lakes (Martínez-Sosa et al., 2021). The distribution pattern of Gahai core sediments is distinctly remarkable compared to that of other lake sediments within the TP, even though they share a common regional origin (Fig. 4). However, its resemblance to the global distribution of brGDGTs in lake sediments is evident. Notably, the calibration developed by Martínez-Sosa et al. (2021) is based on brGDGTs from a global lake dataset.

Using calibration of Martínez-Sosa's et al. (2021), we reconstructed the surface sediment temperature of Gahai lake, resulting in a temperature estimate of 9.4 °C. This reconstructed temperature closely matches the ice-free season temperature recorded by meteorological stations in the Gahai region (8.8 °C for May to September). Furthermore, considering the significant contribution of autochthonous brGDGTs in Gahai lake, we also attempted to reconstruct the Holocene paleotemperature record using previously published lake-specific brGDGT–temperature calibrations (e.g., Günther et al., 2014; Martínez-Sosa et al., 2021; Russell et al., 2018; Sun et al., 2011; Wang et al., 2016). As depicted in Fig. S3, most of these calibrations exhibit qualitatively similar temperature change patterns when applied to the sediment core from Gahai lake. This similarity arises from their shared same principles, just utilizing distinct datasets, resulting in records that display analogous trends but vary in absolute temperatures.

The depth interval of 191–279 cm in the Gahai sediment core represents an interval of rapid allochthonous sedimentation, or alternatively a slump, and therefore the results for the corresponding time interval of 20–15 ka may be unreliable. Thus, our temperature record of months above freezing from the eastern TP spans the past 15 ka, with the average temperature of 4 °C, as shown in Fig. 5a. Within the range of age uncertainties, weak warming occurred during 15–11.8 ka, likely to corresponding to the Bølling–Allerød interstadial. A minor cold reversal occurred during 11.8–10.5 ka, potentially corresponding to the Younger Dryas (YD) event. Notably, the samples collected between 11.8 and 10.5 ka exhibited GDGT concentrations below the detection limit. Therefore, we directly linked the temperature reconstructions at the two aforementioned time points, ∼ 11.8 and ∼ 10.5 ka, resulting in the lowest temperature of this time period appearing around 10.5 ka. This may cause a time lag with the occurrence of the YD event. The temperature record indicates a colder period during 11.5–8.0 ka. During 8.0–3.5 ka, Gahai experienced a stable warm period with the average temperature of ∼ 16.5 °C, after which the temperature decreased gradually. Overall, the maximum temperature dif-

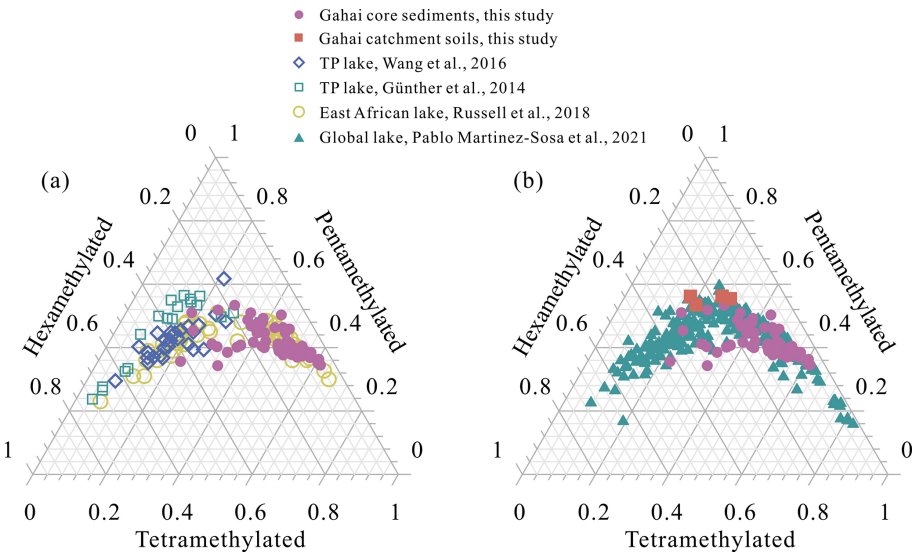

Figure 4. Comparison of the fractional abundances of tetramethylated, pentamethylated, and hexamethylated bGDGTs in sediment core samples from Gahai with lake surface sediments from the TP (Wang et al., 2016; Günther et al., 2014), eastern Africa (Russell et al., 2018), and worldwide (Martínez-Sosa et al., 2021).

ference since 15 ka was ∼ 10 °C. As for the absolute temperature changes since 15 000 years, although some influential studies indicate a warming of approximately 6.1–7 °C from the deglaciation onset to preindustrial times (Tierney et al., 2020; Osman et al., 2021). However, these results are based on global mean sea surface temperatures. Our reconstructed temperature range is about 10 °C, considering the remarkable "elevation-dependent warming" observed in high-altitude regions compared to low-altitude areas (Mountain Research Initiative EDW Working Group, 2015). Thus, this range could be accurate. Nevertheless, we do not rule out the possibility that our temperature reconstruction may exhibit an overestimation. Aside from potential uncertainties associated with the biomarkers themselves, calibrations may also considerably influence the observed amplitude. We examined temperature variations reconstructed using different calibrations (Fig. S3), with the smallest range being 6 °C and the largest being 12 °C. Undoubtedly, further efforts are needed to constrain the inherent uncertainties related to biomarker-based temperature reconstructions.

3.4 Holocene temperature changes on the eastern edge of TP and their origin

Despite the difference in amplitude, the temperature record of MAF from Gahai resembles the pollen record and the pollen-based temperature reconstruction from the same site (Fig. 5) (Wang et al., 2022). However, the brGDGT-based Holocene thermal maximum (HTM) lags the pollen-based reconstruction (Fig. 5a, b). Wang et al. (2022) used a weighted-averaging partial least regression approach to produce a temperature record for Gahai, based on a modern pollen dataset ($n = 731$) from the eastern TP. Assessment of the statistical significance of the pollen-based climate variables for Gahai suggests that the mean July temperature is the most important environmental factor influencing the fossil pollen assemblages. The brGDGTs in Gahai are indicative of summer and autumn temperatures, and the mismatch between the temperature records inferred from brGDGTs and the pollen record may be attributed to the difference between the solar irradiance during June–October and that during July. A detailed analysis of this topic will be undertaken in the subsequent section.

The brGDGT-based temperature record from Gahai confirms the occurrence of a climate optimum in the mid-Holocene on the northeast TP, which is consistent with several other pollen and pollen-reconstructed temperature records from the fringe areas of the Asian summer monsoon (Fig. 6), suggesting that it is a reliable representation of Holocene temperature changes in this region. For example, pollen-based temperature reconstructions from Xingyun lake and Ximen Co on the eastern TP show an early to middle HTM (9–4 ka) and a cooling trend thereafter (Fig. 6c, e) (Wu et al., 2018; Herzschuh et al., 2014; G. Wang et al., 2021). Additionally, lake water temperature reconstructions based on subfossil chironomids from Tiancai lake (Fig. 6f) (E. Zhang et al., 2017, 2019) and alkenones from Qinghai lake (Fig. 6g) (Hou et al., 2016) show the same trends during the past 15 ka, as also shown by other pollen-based temperature records from the TP (Chen et al., 2020). Pollen, chironomids, and alkenones mainly respond to the growing season temperatures in middle and high latitudes, and thus the reconstructed temperature records are consistent with the variations in summer solar irradiance. Similar variations were

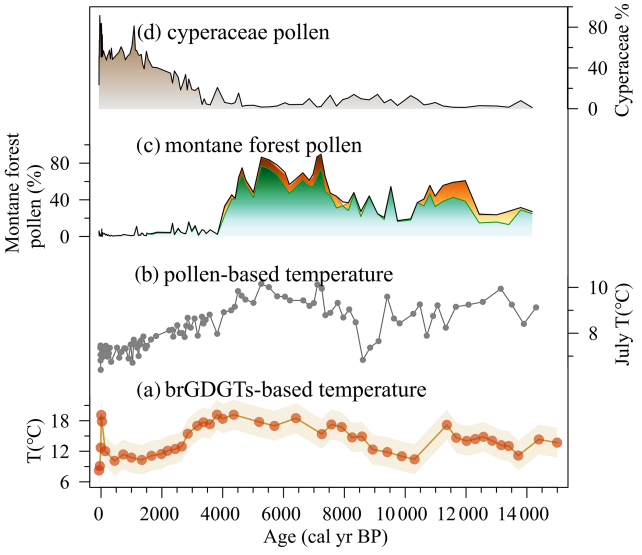

Figure 5. Comparison of multiproxy records from Gahai lake. **(a)** The brGDGT-based MAF (this study). **(b)** Temperature of the warmest month (July) based on pollen assemblages (Wang et al., 2022). **(c, d)** Pollen-reconstructed montane forest (*Pinus*, *Picea*, *Abies*) and Cyperaceae pollen record (Wang et al., 2022).

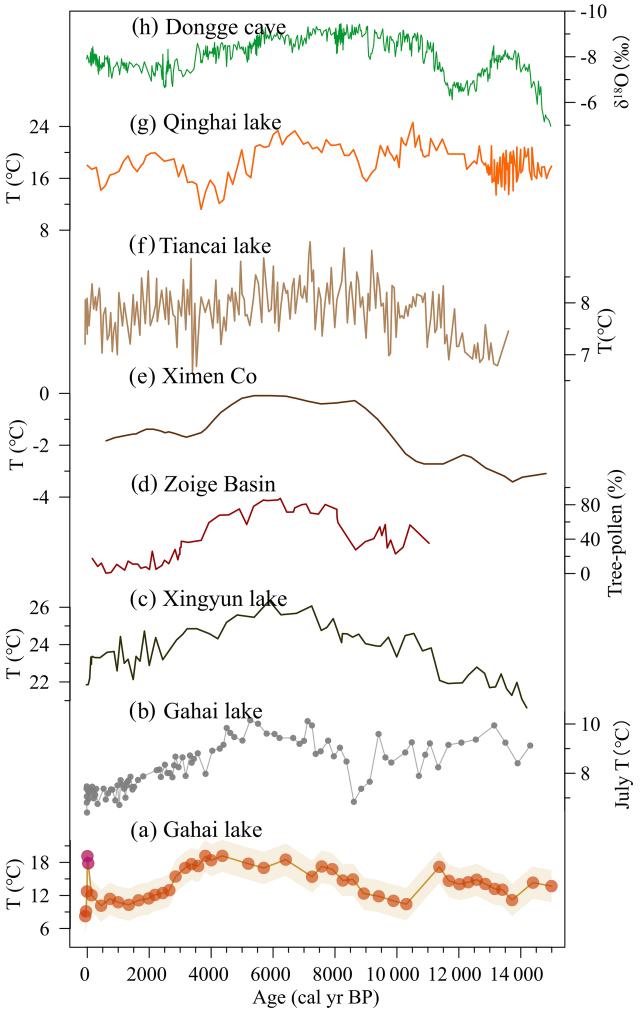

Figure 6. Comparison of temperature at Gahai and other records from the eastern edge of the TP. **(a)** The brGDGT-based MAF at Gahai; the purple dots may indicate unreliable temperature changes influenced by human activities (this study). **(b)** Temperature of the warmest month (July) based on pollen data from Gahai (Wang et al., 2022). **(c)** Pollen-based temperature at Xingyun lake (Wu et al., 2018). **(d)** Tree pollen percentages from the Hongyuan peatland in the southern Zoige basin (Zhou et al., 2010). **(e)** Pollen-based temperature at Ximen Co (Herzschuh et al., 2014). **(f)** Chironomid-based temperature at Tiancai lake (E. Zhang et al., 2017, 2019). **(g)** Alkenone-based temperature at Qinghai lake (Hou et al., 2016). **(h)** Stalagmite δ^{18}O record of Donge cave (Dykoski et al., 2005).

documented in temperature reconstructions at a global scale (Marcott et al., 2013; Cartapanis et al., 2022). Nevertheless, the timing and amplitude of the Gahai temperature fluctuations differ from those of other temperature records from this region (Fig. 6). These discrepancies may be the result of the chronological uncertainties of these records and related to differences in the seasonal and spatial responses to climate forcing and feedbacks.

The temperature record in Gahai during the early Holocene fails to closely track the Northern Hemisphere insolation trend, and there is also a time lag. The pollen-based temperature record for Xingyun lake in southwestern China also shows lower temperatures in the early Holocene (Fig. 6c). The albedo effect caused by the increased cloud cover may be the reason for the early Holocene decrease in summer temperatures (Wu et al., 2018). However, the pollen record from Gahai indicates dry conditions during the early Holocene (Wang et al., 2022), and cloud cover may not be the primary factor responsible for the low temperatures at this time. The melting of Northern Hemisphere ice sheets during the early Holocene would weaken the Atlantic Meridional Overturning Circulation (AMOC) and potentially also the global thermohaline circulation. This would lead to a reduction in the amount of heat transport by the North Atlantic warm current to high-latitude regions and a cooling in middle to high latitudes of the Northern Hemisphere. The persistence of the Laurentide ice sheet into the early Holocene maintained the regional albedo, as well as discharging meltwater into the North Atlantic (Fig. 7d) (Dyke, 2004). Furthermore, the cooling during the early Holocene followed by the warming trend in the mid-Holocene potentially correlates with significant fluctuations in CO_2 concentrations within these intervals (Fig. 7e) (Monnin et al., 2004). In addition, a Holocene temperature simulation showed that global warming was more pronounced when dust factors were excluded from the simulation (Liu et al., 2018). The record of insoluble particles in the Greenland GISP2 ice core indicates relatively high concentrations of atmospheric aerosols in the early Holocene (Zielinski and Mershon, 1997), which would

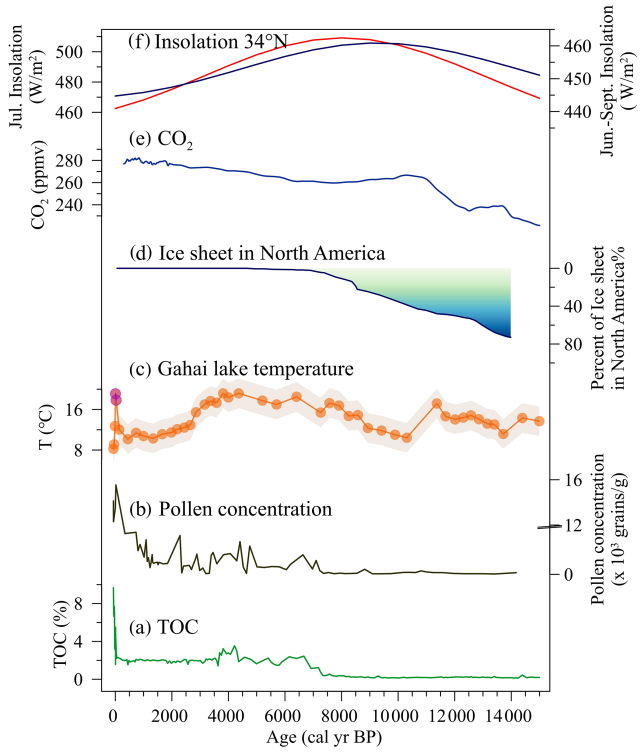

Figure 7. Temperature fluctuations and forcing factors during the Holocene. **(a, b)** TOC (total organic carbon) content and pollen concentrations from Gahai (Wang et al., 2022). **(c)** BrGDGT-based MAF from Gahai, the purple dots may indicate unreliable temperature changes influenced by human activities (this study). **(d)** Percentage of the remnant Laurentide ice sheet in North America relative to the Last Glacial Maximum (Dyke, 2004). **(e)** Varaition of atmospheric CO_2 content (Monnin et al., 2004). **(f)** Mean insolation during July ($W\,m^{-2}$) (navy blue curve) and mean insolation during ice-free months ($W\,m^{-2}$) at 34° N (red curve) (Berger and Loutre, 1991; Berger et al., 2010).

give weakened summer solar irradiation via radiative feedback, leading to the cool temperatures during this period. In essence, temperature, especially seasonal variations like the Gahai ice-free temperature in the eastern TP, is influenced by multifaceted factors including astronomical forcing, CO_2, and ice sheets. Temperature exhibits varied sensitivities in response to these factors, while both insolation and CO_2 exert considerable and favorable impacts on summer temperature patterns (Lyu and Yin, 2022). These factors may together have caused the early Holocene temperature decline at Gahai lake, which slightly delayed the onset of the Holocene Warm Period.

A notable and rapid temperature increase is evident at Gahai in recent decades, which differs from the other records (Fig. 7c). Moreover, there are notable increases in pollen concentration, TOC, and TN (Fig. 7a, b) in the Gahai sediment core, indicating intensive local human activities like grazing and tourism, which may be the primary cause of the environmental changes in this region (Wang et al., 2022). This intensive human activity may have reduced the ability of the brGDGTs to record the natural temperature background. These observations emphasize the important impact of human activities on climate proxies and the need to carefully consider their effect on temperature reconstructions.

3.5 Spatiotemporal pattern of brGDGT-based TP temperatures

In addition to comparing the Gahai temperature with the summer temperature records from the eastern TP and its surrounding areas, we compiled and reviewed published Holocene brGDGT-based quantitative temperature records from across the TP. As shown in Fig. 8, with the increasing number of these records for the TP, the differences between the results have become more pronounced. The brGDGTs records from lakes in the central and western parts of the plateau show higher temperatures in the early and late Holocene, and lower temperatures in the middle Holocene (M. D. Wang et al., 2021; Li et al., 2017; He et al., 2020), while the brGDGTs records from lakes in the southern and south-eastern parts of the TP show a warming trend throughout the Holocene (Sun et al., 2022; Feng et al., 2022). In addition, brGDGTs in Cuoqia lake and Tingming lake, on the southeastern TP, recorded the ice-free season temperature, which was relatively stable during the Holocene (Sun et al., 2021; C. Zhang et al., 2022). However, our temperature record from Gahai is different from the above records and resembles summer temperature changes during the Holocene (Chen et al., 2020). This is because the brGDGTs record from Gahai lake represents warm-season temperatures, which adds to its reliability.

We suggest that the complexity of Holocene temperature patterns recorded by brGDGTs in TP lakes is primarily due to the ambiguity of brGDGTs in these lakes, as well as to the spatial heterogeneity of climate change across the TP. This ambiguity can be attributed to several factors. First, the origin of brGDGTs in lakes remains an uncertain factor in temperature reconstruction. An increasing number of studies indicate the occurrence of a remarkable amount of autochthonous brGDGTs in lakes, but their abundance in soil can also affect the distribution of brGDGTs in lakes due to their supply via soil erosion (e.g., Tierney and Russell, 2009; Weber et al., 2015; Wang et al., 2023). Therefore, it is important to conduct detailed modern process studies to accurately assess the sources of brGDGTs in lakes, especially with regard to evaluating the proportion of autochthonous brGDGTs (Wang et al., 2023; Martin et al., 2020). Second, brGDGTs may show a seasonal signal. Current brGDGTs–temperature calibrations for lakes reflect the annual average temperature (Sun et al., 2011; De Jonge et al., 2014), as well as the growing season temperature (Sun et al., 2011; Dang et al., 2018) and the ice-free season temperature (Martínez-Sosa et al., 2021; C. Zhang et al., 2022). Thus, there is no consensus

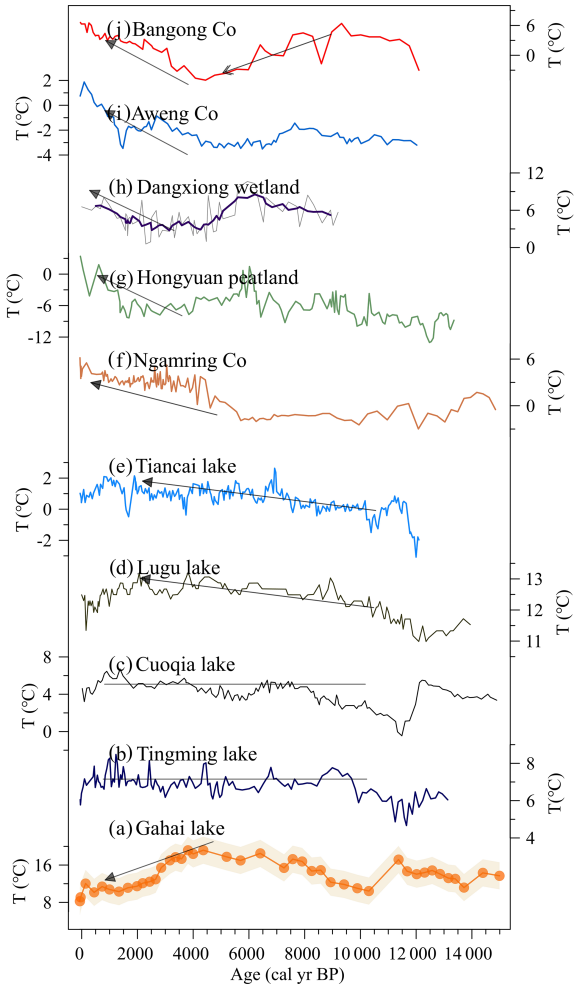

Figure 8. Comparison of Holocene temperature based on brGDGTs at Gahai **(a)** and other records from around the TP. Reconstructed ice-free season temperatures from **(b)** Tingming lake (Sun et al., 2021) and **(c)** Cuoqia lake (C. Zhang et al., 2022). Reconstructed annual temperature from **(d)** Lugu lake (C. Zhao et al., 2021), **(e)** Tiancai lake (Feng et al., 2022), **(f)** Ngamring Co (Sun et al., 2022), **(g)** Hongyuan peatland (Yan et al., 2021), **(h)** Dangxiong wetland (Cheung et al., 2017), **(i)** Aweng Co (Li et al., 2017), and **(j)** Bangong Co (M. D. Wang et al., 2021).

regarding whether the brGDGTs have a seasonal bias, and it is necessary to conduct continuous, high-resolution seasonal investigations of lakes on the TP to comprehensively elucidate the seasonal characteristics of brGDGTs. This can enhance the accuracy of regional temperature reconstruction and may help reconcile the complex temperature patterns observed on the TP. Third, the factors affecting the distribution of brGDGTs in lakes are complex, including not only temperature, pH, and salinity but also oxygen content, water depth, and so on (H. Wang et al., 2021; Wang et al., 2016). The distribution of brGDGTs in lakes is significantly influenced by the hydrological and physical properties of the lakes, and thus it is necessary to attain a more comprehensive understanding of the characteristics of the lakes in the study area and their effects on brGDGTs. Fourth, different brGDGT–temperature calibrations may lead to markable differences in both the amplitude and trend of temperature from the same dataset (Wang et al., 2016; Feng et al., 2019). One reason for this is the deviation between in situ measured temperature and atmospheric temperature (Wang et al., 2020). Thus, selecting an appropriate calibration and attempting to establish a brGDGTs–in situ temperature calibration are effective means of enhancing the reliability of brGDGT-based temperature reconstructions.

4 Conclusions

We present a quantitative, brGDGT-based seasonal paleotemperature record over the last 15 ka from the sediments of a shallow lake on the eastern TP. Our reconstruction resembles the summer temperature trend, with the Holocene Thermal Maximum occurring during 8–3.5 ka. There is a lag between our brGDGT-based reconstruction and pollen-based temperature recorded in the same sediment core, indicating a seasonal bias between different proxies. Since 3.5 ka, the temperature decreased gradually, and the surficial sediments reliably recorded the warm-season temperature during the current period in the Gahai lake region. However, intensive local human activity during the last century has affected the distribution of brGDGTs, resulting in temperature deviations recorded by brGDGTs. The implementation of environmental protection policies has reduced this anthropogenic signal. Our findings help us to better understand the seasonal signal of brGDGTs in shallow lakes and provide important data for improving projections of terrestrial climate change at high elevations.

We also investigated previously published brGDGT-based Holocene temperature records on the TP to determine the pattern of brGDGT-based temperature changes and the possible causes of the differences between reconstructions. We emphasize the need for the careful examination of both the source and behavior of these compounds in lacustrine environments and lake status, prior to the application of brGDGTs proxies in paleolimnological reconstruction.

Data availability. The data used in this study can be obtained from the corresponding author Juzhi Hou (houjz@itpcas.ac.cn).

Supplement. The supplement related to this article is available online at: https://doi.org/10.5194/cp-20-335-2024-supplement.

Author contributions. XH did the experiments, analyzed the data, and wrote the manuscript. NW, ZS, KY, and XC participated in sample collecting and data analysis. JH designed the study and

led the interpretation. All authors commented on and improved the manuscript.

Competing interests. The contact author has declared that none of the authors has any competing interests.

Disclaimer. Publisher's note: Copernicus Publications remains neutral with regard to jurisdictional claims made in the text, published maps, institutional affiliations, or any other geographical representation in this paper. While Copernicus Publications makes every effort to include appropriate place names, the final responsibility lies with the authors.

Acknowledgements. This work was financially supported by the National Natural Science Foundation of China (42025103, 41877459) and the Second Tibetan Plateau Scientific Expedition and Research (2019QZKK0601). We are grateful to the two anonymous reviewers and handling editor Qiuzhen Yin for their valuable comments that significantly improved the quality of the manuscript. We would like to thank Jan Bloemendal for the help with language editing.

Financial support. This research has been supported by the National Natural Science Foundation of China (grant nos. 42025103, 41877459) and the Second Tibetan Plateau Scientific Expedition and Research (grant no. 2019QZKK0601).

Review statement. This paper was edited by Qiuzhen Yin and reviewed by two anonymous referees.

References

Appleby, P. G.: Chronostratigraphic techniques in recent sediments, in: Tracking Environmental Change Using Lake Sediments, Springer, 171–203, ISBN 978-0-7923-6482-5, 2002.

Berger, A. and Loutre, M. F.: Insolation values for the climate of the last 10 000 000 years, Quaternary Sci. Rev., 10, 297–317, https://doi.org/10.1016/0277-3791(91)90033-q, 1991.

Berger, A., Loutre, M. F., and Yin, Q. Z.: Total irradiation during any time interval of the year using elliptic integrals, Quaternary Sci. Rev., 29, 1968–1982, https://doi.org/10.1016/j.quascirev.2010.05.007, 2010.

Blaauw, M. and Andres Christen, J.: Flexible Paleoclimate Age-Depth Models Using an Autoregressive Gamma Process, Bayesian Anal., 6, 457–474, https://doi.org/10.1214/ba/1339616472, 2011.

Bova, S., Rosenthal, Y., Liu, Z., Godad, S. P., and Yan, M.: Seasonal origin of the thermal maxima at the Holocene and the last interglacial, Nature, 589, 548–553, https://doi.org/10.1038/s41586-020-03155-x, 2021.

Buckles, L. K., Weijers, J. W. H., Verschuren, D., and Damste, J. S. S.: Sources of core and intact branched tetraether membrane lipids in the lacustrine environment: Anatomy of Lake Challa and its catchment, equatorial East Africa, Geochim. Cosmochim. Ac., 140, 106–126, https://doi.org/10.1016/j.gca.2014.04.042, 2014.

Cao, J., Rao, Z., Shi, F., and Jia, G.: Ice formation on lake surfaces in winter causes warm-season bias of lacustrine brGDGT temperature estimates, Biogeosciences, 17, 2521–2536, https://doi.org/10.5194/bg-17-2521-2020, 2020.

Cartapanis, O., Jonkers, L., Moffa-Sanchez, P., Jaccard, S. L., and de Vernal, A.: Complex spatio-temporal structure of the Holocene Thermal Maximum, Nat. Commun., 13, 5662, https://doi.org/10.1038/s41467-022-33362-1, 2022.

Chen, D., Xu, B., Yao, T., Guo, Z., Cui, P., Chen, F., Zhang, R., Zhang, X., Zhang, Y., Fan, J., Hou, Z., and Zhang, T.: Assessment of past, present and future environmental changes on the Tibetan Plateau, Chinese Sci. Bull., 60, 3025–3035, 2015.

Chen, F., Yu, Z., Yang, M., Ito, E., Wang, S., Madsen, D. B., Huang, X., Zhao, Y., Sato, T., Birks, H. J. B., Boomer, I., Chen, J., An, C., and Wünnemann, B.: Holocene moisture evolution in arid central Asia and its out-of-phase relationship with Asian monsoon history, Quaternary Sci. Rev., 27, 351–364, https://doi.org/10.1016/j.quascirev.2007.10.017, 2008.

Chen, F., Zhang, J., Liu, J., Cao, X., Hou, J., Zhu, L., Xu, X., Liu, X., Wang, M., Wu, D., Huang, L., Zeng, T., Zhang, S., Huang, W., Zhang, X., and Yang, K.: Climate change, vegetation history, and landscape responses on the Tibetan Plateau during the Holocene: A comprehensive review, Quaternary Sci. Rev., 243, 106444, https://doi.org/10.1016/j.quascirev.2020.106444, 2020.

Chen, Y., Zheng, F., Yang, H., Yang, W., Wu, R., Liu, X., Liang, H., Chen, H., Pei, H., Zhang, C., Pancost, R. D., and Zeng, Z.: The production of diverse brGDGTs by an Acidobacterium providing a physiological basis for paleoclimate proxies, Geochim. Cosmochim. Ac., 337, 155–165, https://doi.org/10.1016/j.gca.2022.08.033, 2022.

Cheung, M.-C., Zong, Y., Zheng, Z., Liu, Z., and Aitchison, J. C.: Holocene temperature and precipitation variability on the central Tibetan Plateau revealed by multiple palaeo-climatic proxy records from an alpine wetland sequence, Holocene, 27, 1669–1681, https://doi.org/10.1177/0959683617702225, 2017.

Crampton-Flood, E. D., Tierney, J. E., Peterse, F., Kirkels, F. M. S. A., and Damste, J. S. S.: BayMBT: A Bayesian calibration model for branched glycerol dialkyl glycerol tetraethers in soils and peats, Geochim. Cosmochim. Ac., 268, 142–159, https://doi.org/10.1016/j.gca.2019.09.043, 2020.

Dang, X., Ding, W., Yang, H., Pancost, R. D., Naafs, B. D. A., Xue, J., Lin, X., Lu, J., and Xie, S.: Different temperature dependence of the bacterial brGDGT isomers in 35 Chinese lake sediments compared to that in soils, Org. Geochem., 119, 72–79, https://doi.org/10.1016/j.orggeochem.2018.02.008, 2018.

De Jonge, C., Hopmans, E. C., Zell, C. I., Kim, J.-H., Schouten, S., and Sinninghe Damsté, J. S.: Occurrence and abundance of 6-methyl branched glycerol dialkyl glycerol tetraethers in soils: Implications for palaeoclimate reconstruction, Geochim. Cosmochim. Ac., 141, 97–112, https://doi.org/10.1016/j.gca.2014.06.013, 2014.

Ding, S., Xu, Y., Wang, Y., He, Y., Hou, J., Chen, L., and He, J.-S.: Distribution of branched glycerol dialkyl glycerol tetraethers in surface soils of the Qinghai–Tibetan Plateau: implications of brGDGTs-based proxies in cold and dry regions, Biogeo-

sciences, 12, 3141–3151, https://doi.org/10.5194/bg-12-3141-2015, 2015.

Dong, Y., Wu, N., Li, F., Zhang, D., Zhang, Y., Shen, C., and Lu, H.: The Holocene temperature conundrum answered by mollusk records from East Asia, Nat. Commun., 13, 5153, https://doi.org/10.1038/s41467-022-32506-7, 2022.

Dyke, A. S.: An outline of North American deglaciation with emphasis on central and northern Canada, Quaternary Glaciations-Extent and Chronology, Pt 2: North America, edited by: Ehlers, J. and Gibbard, P. L., Elsevier, Amsterdam, the Netherlands, 373–424, https://doi.org/10.1016/s1571-0866(04)80209-4, 2004.

Dykoski, C. A., Edwards, R. L., Cheng, H., Yuan, D. X., Cai, Y. J., Zhang, M. L., Lin, Y. S., Qing, J. M., An, Z. S., and Revenaugh, J.: A high-resolution, absolute-dated Holocene and deglacial Asian monsoon record from Dongge Cave, China, Earth Planet. Sc. Lett., 233, 71–86, https://doi.org/10.1016/j.epsl.2005.01.036, 2005.

Feng, X., Zhao, C., D'Andrea, W. J., Liang, J., Zhou, A., and Shen, J.: Temperature fluctuations during the Common Era in subtropical southwestern China inferred from brGDGTs in a remote alpine lake, Earth Planet. Sc. Lett., 510, 26–36, https://doi.org/10.1016/j.epsl.2018.12.028, 2019.

Feng, X., Zhao, C., D'Andrea, W. J., Hou, J., Yang, X., Xiao, X., Shen, J., Duan, Y., and Chen, F.: Evidence for a Relatively Warm Mid-to Late Holocene on the Southeastern Tibetan Plateau, Geophys. Res. Lett., 49, e2022GL098740, https://doi.org/10.1029/2022gl098740, 2022.

Günther, F., Thiele, A., Gleixner, G., Xu, B., Yao, T., and Schouten, S.: Distribution of bacterial and archaeal ether lipids in soils and surface sediments of Tibetan lakes: Implications for GDGT-based proxies in saline high mountain lakes, Org. Geochem., 67, 19–30, https://doi.org/10.1016/j.orggeochem.2013.11.014, 2014.

Halamka, T. A., Raberg, J. H., McFarlin, J. M., Younkin, A. D., Mulligan, C., Liu, X. L., and Kopf, S. H.: Production of diverse brGDGTs by Acidobacterium *Solibacter usitatus* in response to temperature, pH, and O_2 provides a culturing perspective on brGDGT proxies and biosynthesis, Geobiology, 21, 102–118, https://doi.org/10.1111/gbi.12525, 2022.

He, Y., Hou, J., Wang, M., Li, X., Liang, J., Xie, S., and Jin, Y.: Temperature Variation on the Central Tibetan Plateau Revealed by Glycerol Dialkyl Glycerol Tetraethers From the Sediment Record of Lake Linggo Co Since the Last Deglaciation, Front. Earth Sci., 8, 574206, https://doi.org/10.3389/feart.2020.574206, 2020.

Herzschuh, U., Borkowski, J., Schewe, J., Mischke, S., and Tian, F.: Moisture-advection feedback supports strong early-to-mid Holocene monsoon climate on the eastern Tibetan Plateau as inferred from a pollen-based reconstruction, Paleogeogr. Paleocl., 402, 44–54, https://doi.org/10.1016/j.palaeo.2014.02.022, 2014.

Hou, J., D'Andrea, W. J., and Liu, Z.: The influence of ^{14}C reservoir age on interpretation of paleolimnological records from the Tibetan Plateau, Quaternary Sci. Rev., 48, 67–79, https://doi.org/10.1016/j.quascirev.2012.06.008, 2012.

Hou, J., Huang, Y., Zhao, J., Liu, Z., Colman, S., and An, Z.: Large Holocene summer temperature oscillations and impact on the peopling of the northeastern Tibetan Plateau, Geophys. Res. Lett., 43, 1323–1330, https://doi.org/10.1002/2015gl067317, 2016.

Hou, J., Li, C., and Lee, S.: The temperature record of the Holocene: progress and controversies, Sci. Bull., 64, 565–566, https://doi.org/10.1016/j.scib.2019.02.012, 2019.

Huguet, C., Hopmans, E. C., Febo-Ayala, W., Thompson, D. H., Sinninghe Damsté, J. S., and Schouten, S.: An improved method to determine the absolute abundance of glycerol dibiphytanyl glycerol tetraether lipids, Org. Geochem., 37, 1036–1041, https://doi.org/10.1016/j.orggeochem.2006.05.008, 2006.

Kuang, X. and Jiao, J. J.: Review on climate change on the Tibetan Plateau during the last half century, J. Geophys. Res.-Atmos., 121, 3979–4007, https://doi.org/10.1002/2015jd024728, 2016.

Li, X., Wang, M., Zhang, Y., Lei, L., and Hou, J.: Holocene climatic and environmental change on the western Tibetan Plateau revealed by glycerol dialkyl glycerol tetraethers and leaf wax deuterium-to-hydrogen ratios at Aweng Co, Quaternary Res., 87, 455–467, https://doi.org/10.1017/qua.2017.9, 2017.

Liang, W. and Luo, A.: Luqu County Annals, Gansu Culture Press, Lanzhou, 71 pp., 2006 (in Chinese).

Liu, Y., Zhang, M., Liu, Z., Xia, Y., Huang, Y., Peng, Y., and Zhu, J.: A Possible Role of Dust in Resolving the Holocene Temperature Conundrum, Sci. Rep., 8, 4434, https://doi.org/10.1038/s41598-018-22841-5, 2018.

Liu, Z. Y., Zhu, J., Rosenthal, Y., Zhang, X., Otto-Bliesner, B. L., Timmermann, A., Smith, R. S., Lohmann, G., Zheng, W. P., and Timm, O. E.: The Holocene temperature conundrum, P. Natl. Acad. Sci. USA, 111, E3501–E3505, https://doi.org/10.1073/pnas.1407229111, 2014.

Loomis, S. E., Russell, J. M., Heureux, A. M., D'Andrea, W. J., and Sinninghe Damsté, J. S.: Seasonal variability of branched glycerol dialkyl glycerol tetraethers (brGDGTs) in a temperate lake system, Geochim. Cosmochim. Ac., 144, 173–187, https://doi.org/10.1016/j.gca.2014.08.027, 2014.

Lu, H., Wu, N., Liu, K.-B., Zhu, L., Yang, X., Yao, T., Wang, L., Li, Q., Liu, X., Shen, C., Li, X., Tong, G., and Jiang, H.: Modern pollen distributions in Qinghai-Tibetan Plateau and the development of transfer functions for reconstructing Holocene environmental changes, Quaternary Sci. Rev., 30, 947–966, https://doi.org/10.1016/j.quascirev.2011.01.008, 2011.

Lyu, A. and Yin, Q. Z.: The spatial-temporal patterns of East Asian climate in response to insolation, CO_2 and ice sheets during MIS-5, Quaternary Sci. Rev., 293, 107689, https://doi.org/10.1016/j.quascirev.2022.107689, 2022.

Ma, W., Li, G., Song, J., Yan, L., and Wu, L.: Effect of Vegetation Degradation on Soil Organic Carbon Pool and Carbon Pool Management Index in the Gahai Wetland,China, Acta Agrestia Sinica, 27, 687–694, 2019.

Marcott, S. A., Shakun, J. D., Clark, P. U., and Mix, A. C.: A Reconstruction of Regional and Global Temperature for the Past 11,300 Years, Science, 339, 1198–1201, https://doi.org/10.1126/science.1228026, 2013.

Marsicek, J., Shuman, B. N., Bartlein, P. J., Shafer, S. L., and Brewer, S.: Reconciling divergent trends and millennial variations in Holocene temperatures, Nature, 554, 92–96, https://doi.org/10.1038/nature25464, 2018.

Martin, C., Ménot, G., Thouveny, N., Peyron, O., Andrieu-Ponel, V., Montade, V., Davtian, N., Reille, M., and Bard, E.: Early Holocene Thermal Maximum recorded by branched tetraethers and pollen in Western Europe (Mas-

sif Central, France), Quaternary Sci. Rev., 228, 106109, https://doi.org/10.1016/j.quascirev.2019.106109, 2020.

Martínez-Sosa, P., Tierney, J. E., Stefanescu, I. C., Dearing Crampton-Flood, E., Shuman, B. N., and Routson, C.: A global Bayesian temperature calibration for lacustrine brGDGTs, Geochim. Cosmochim. Ac., 305, 87–105, https://doi.org/10.1016/j.gca.2021.04.038, 2021.

Monnin, E., Steig, E. J., Siegenthaler, U., Kawamura, K., Schwander, J., Stauffer, B., Stocker, T. F., Morse, D. L., Barnola, J. M., Bellier, B., Raynaud, D., and Fischer, H.: Evidence for substantial accumulation rate variability in Antarctica during the Holocene, through synchronization of CO_2 in the Taylor Dome, Dome C and DML ice cores, Earth Planet. Sc. Lett., 224, 45–54, https://doi.org/10.1016/j.epsl.2004.05.007, 2004.

Moser, K. A., Baron, J. S., Brahney, J., Oleksy, I. A., Saros, J. E., Hundey, E. J., Sadro, S., Kopáček, J., Sommaruga, R., Kainz, M. J., Strecker, A. L., Chandra, S., Walters, D. M., Preston, D. L., Michelutti, N., Lepori, F., Spaulding, S. A., Christianson, K. R., Melack, J. M., and Smol, J. P.: Mountain lakes: Eyes on global environmental change, Glob. Planet Change, 178, 77–95, https://doi.org/10.1016/j.gloplacha.2019.04.001, 2019.

Mountain Research Initiative EDW Working Group: Elevation-dependent warming in mountain regions of the world, Nat. Clim. Change, 5, 424-430, https://doi.org/10.1038/nclimate2563, 2015.

Opitz, S., Zhang, C., Herzschuh, U., and Mischke, S.: Climate variability on the south-eastern Tibetan Plateau since the Lateglacial based on a multiproxy approach from Lake Naleng – comparing pollen and non-pollen signals, Quaternary Sci. Rev., 115, 112–122, https://doi.org/10.1016/j.quascirev.2015.03.011, 2015.

Osman, M. B., Tierney, J. E., Zhu, J., Tardif, R., Hakim, G. J., King, J., and Poulsen, C. J.: Globally resolved surface temperatures since the Last Glacial Maximum, Nature, 599, 239–244, https://doi.org/10.1038/s41586-021-03984-4, 2021.

Pang, H., Hou, S., Zhang, W., Wu, S., Jenk, T. M., Schwikowski, M., and Jouzel, J.: Temperature Trends in the Northwestern Tibetan Plateau Constrained by Ice Core Water Isotopes Over the Past 7,000 Years, J. Geophys. Res.-Atmos., 125, https://doi.org/10.1029/2020jd032560, 2020.

Qiu, J.: The third pole, Nature, 454, 393–396, https://doi.org/10.1038/454393a, 2008.

Russell, J. M., Hopmans, E. C., Loomis, S. E., Liang, J., and Sinninghe Damsté, J. S.: Distributions of 5- and 6-methyl branched glycerol dialkyl glycerol tetraethers (brGDGTs) in East African lake sediment: Effects of temperature, pH, and new lacustrine paleotemperature calibrations, Org. Geochem., 117, 56–69, https://doi.org/10.1016/j.orggeochem.2017.12.003, 2018.

Sinninghe Damsté, J. S., Hopmans, E. C., Pancost, R. D., Schouten, S., and Geenevasen, J. A. J.: Newly discovered non-isoprenoid glycerol dialkyl glycerol tetraether lipids in sediments, Chem. Commun., 1683–1684, https://doi.org/10.1039/b004517i, 2000.

Sinninghe Damsté, J. S., Ossebaar, J., Abbas, B., Schouten, S., and Verschuren, D.: Fluxes and distribution of tetraether lipids in an equatorial African lake: Constraints on the application of the TEX_{86} palaeothermometer and BIT index in lacustrine settings, Geochim. Cosmochim. Ac., 73, 4232–4249, https://doi.org/10.1016/j.gca.2009.04.022, 2009.

Sun, Q., Chu, G., Liu, M., Xie, M., Li, S., Ling, Y., Wang, X., Shi, L., Jia, G., and Lü, H.: Distributions and temperature dependence of branched glycerol dialkyl glycerol tetraethers in recent lacustrine sediments from China and Nepal, J. Geophys. Res., 116, G01008, https://doi.org/10.1029/2010jg001365, 2011.

Sun, X., Zhao, C., Zhang, C., Feng, X., Yan, T., Yang, X., and Shen, J.: Seasonality in Holocene Temperature Reconstructions in Southwestern China, Paleoceanogr. Paleocl., 36, e2020PA004025, https://doi.org/10.1029/2020pa004025, 2021.

Sun, Z., Hou, X., Ji, K., Yuan, K., Li, C., Wang, M., and Hou, J.: Potential winter-season bias of annual temperature variations in monsoonal Tibetan Plateau since the last deglaciation, Quaternary Sci. Rev., 292, 107690, https://doi.org/10.1016/j.quascirev.2022.107690, 2022.

Thompson, L. G., Yao, T., Davis, M. E., Henderson, K. A., MosleyThompson, E., Lin, P. N., Beer, J., Synal, H. A., ColeDai, J., and Bolzan, J. F.: Tropical climate instability: The last glacial cycle from a Qinghai-Tibetan ice core, Science, 276, 1821–1825, https://doi.org/10.1126/science.276.5320.1821, 1997.

Tierney, J. E. and Russell, J. M.: Distributions of branched GDGTs in a tropical lake system: Implications for lacustrine application of the MBT/CBT paleoproxy, Org. Geochem., 40, 1032–1036, https://doi.org/10.1016/j.orggeochem.2009.04.014, 2009.

Tierney, J. E., Russell, J. M., Eggermont, H., Hopmans, E. C., Verschuren, D., and Sinninghe Damsté, J. S.: Environmental controls on branched tetraether lipid distributions in tropical East African lake sediments, Geochim. Cosmochim. Ac., 74, 4902–4918, https://doi.org/10.1016/j.gca.2010.06.002, 2010.

Tierney, J. E., Zhu, J., King, J., Malevich, S. B., Hakim, G. J., and Poulsen, C. J.: Glacial cooling and climate sensitivity revisited, Nature, 584, 569–573, https://doi.org/10.1038/s41586-020-2617-x, 2020.

van Bree, L. G. J., Peterse, F., Baxter, A. J., De Crop, W., van Grinsven, S., Villanueva, L., Verschuren, D., and Sinninghe Damsté, J. S.: Seasonal variability and sources of in situ brGDGT production in a permanently stratified African crater lake, Biogeosciences, 17, 5443–5463, https://doi.org/10.5194/bg-17-5443-2020, 2020.

Wang, G., Wang, Y., Wei, Z., He, W., Ma, X., and Zhang, T.: Reconstruction of temperature and precipitation spanning the past 28 kyr based on branched tetraether lipids from Qionghai Lake, southwestern China, Paleogeogr. Paleocl., 562, 110094, https://doi.org/10.1016/j.palaeo.2020.110094, 2021.

Wang, H., An, Z., Lu, H., Zhao, Z., and Liu, W.: Calibrating bacterial tetraether distributions towards in situ soil temperature and application to a loess-paleosol sequence, Quaternary Sci. Rev., 231, 106172, https://doi.org/10.1016/j.quascirev.2020.106172, 2020.

Wang, H., Liu, W., He, Y., Zhou, A., Zhao, H., Liu, H., Cao, Y., Hu, J., Meng, B., Jiang, J., Kolpakova, M., Krivonogov, S., and Liu, Z.: Salinity-controlled isomerization of lacustrine brGDGTs impacts the associated MBT'_{5ME} terrestrial temperature index, Geochim. Cosmochim. Ac., 305, 33–48, https://doi.org/10.1016/j.gca.2021.05.004, 2021.

Wang, H., Chen, W., Zhao, H., Cao, Y., Hu, J., Zhao, Z., Cai, Z., Wu, S., Liu, Z., and Liu, W.: Biomarker-based quantitative constraints on maximal soil-derived brGDGTs in modern lake sediments, Earth Planet. Sc. Lett., 602, 117947, https://doi.org/10.1016/j.epsl.2022.117947, 2023.

Wang, M., Liang, J., Hou, J., and Hu, L.: Distribution of GDGTs in lake surface sediments on the Tibetan Plateau and

its influencing factors, Sci. China Earth Sci., 59, 961–974, https://doi.org/10.1007/s11430-015-5214-3, 2016.

Wang, M. D., Hou, J. Z., Duan, Y. W., Chen, J. H., Li, X. M., He, Y., Lee, S. Y., and Chen, F. H.: Internal feedbacks forced Middle Holocene cooling on the Qinghai-Tibetan Plateau, Boreas, 50, 1116–1130, https://doi.org/10.1111/bor.12531, 2021.

Wang, N., Liu, L., Hou, X., Zhang, Y., Wei, H., and Cao, X.: Palynological evidence reveals an arid early Holocene for the northeast Tibetan Plateau, Clim. Past, 18, 2381–2399, https://doi.org/10.5194/cp-18-2381-2022, 2022.

Weber, Y., De Jonge, C., Rijpstra, W. I. C., Hopmans, E. C., Stadnitskaia, A., Schubert, C. J., Lehmann, M. F., Sinninghe Damsté, J. S., and Niemann, H.: Identification and carbon isotope composition of a novel branched GDGT isomer in lake sediments: Evidence for lacustrine branched GDGT production, Geochim. Cosmochim. Ac., 154, 118–129, https://doi.org/10.1016/j.gca.2015.01.032, 2015.

Weber, Y., Sinninghe Damste, J. S., Zopfi, J., De Jonge, C., Gilli, A., Schubert, C. J., Lepori, F., Lehmann, M. F., and Niemann, H.: Redox-dependent niche differentiation provides evidence for multiple bacterial sources of glycerol tetraether lipids in lakes, P. Natl. Acad. Sci. USA, 115, 10926–10931, https://doi.org/10.1073/pnas.1805186115, 2018.

Weijers, J. W. H., Schouten, S., van den Donker, J. C., Hopmans, E. C., and Sinninghe Damsté, J. S.: Environmental controls on bacterial tetraether membrane lipid distribution in soils, Geochim. Cosmochim. Ac., 71, 703–713, https://doi.org/10.1016/j.gca.2006.10.003, 2007.

Woltering, M., Werne, J. P., Kish, J. L., Hicks, R., Sinninghe Damsté, J. S., and Schouten, S.: Vertical and temporal variability in concentration and distribution of thaumarchaeotal tetraether lipids in Lake Superior and the implications for the application of the TEX_{86} temperature proxy, Geochim. Cosmochim. Ac., 87, 136–153, https://doi.org/10.1016/j.gca.2012.03.024, 2012.

Wu, D., Chen, X., Lv, F., Brenner, M., Curtis, J., Zhou, A., Chen, J., Abbott, M., Yu, J., and Chen, F.: Decoupled early Holocene summer temperature and monsoon precipitation in southwest China, Quaternary Sci. Rev., 193, 54–67, https://doi.org/10.1016/j.quascirev.2018.05.038, 2018.

Wu, J., Yang, H., Pancost, R. D., Naafs, B. D. A., Qian, S., Dang, X., Sun, H., Pei, H., Wang, R., Zhao, S., and Xie, S.: Variations in dissolved O_2 in a Chinese lake drive changes in microbial communities and impact sedimentary GDGT distributions, Chem. Geol., 579, 120348, https://doi.org/10.1016/j.chemgeo.2021.120348, 2021.

Yan, T., Zhao, C., Yan, H., Shi, G., Sun, X., Zhang, C., Feng, X., and Leng, C.: Elevational differences in Holocene thermal maximum revealed by quantitative temperature reconstructions at $\sim 30°$ N on eastern Tibetan Plateau, Paleogeogr. Paleocl., 570, 110364, https://doi.org/10.1016/j.palaeo.2021.110364, 2021.

Yao, T., Bolch, T., Chen, D., Gao, J., Immerzeel, W., Piao, S., Su, F., Thompson, L., Wada, Y., Wang, L., Wang, T., Wu, G., Xu, B., Yang, W., Zhang, G., and Zhao, P.: The imbalance of the Asian water tower, Nat. Rev. Earth Environ., 3, 618–632, https://doi.org/10.1038/s43017-022-00299-4, 2022.

Zhang, C., Zhao, C., Yu, S.-Y., Yang, X., Cheng, J., Zhang, X., Xue, B., Shen, J., and Chen, F.: Seasonal imprint of Holocene temperature reconstruction on the Tibetan Plateau, Earth-Sci. Rev., 226, 103927, https://doi.org/10.1016/j.earscirev.2022.103927, 2022.

Zhang, E., Chang, J., Cao, Y., Sun, W., Shulmeister, J., Tang, H., Langdon, P. G., Yang, X., and Shen, J.: Holocene high-resolution quantitative summer temperature reconstruction based on subfossil chironomids from the southeast margin of the Qinghai-Tibetan Plateau, Quaternary Sci. Rev., 165, 1–12, https://doi.org/10.1016/j.quascirev.2017.04.008, 2017.

Zhang, E., Chang, J., Shulmeister, J., Langdon, P., Sun, W., Cao, Y., Yang, X., and Shen, J.: Summer temperature fluctuations in Southwestern China during the end of the LGM and the last deglaciation, Earth Planet. Sc. Lett., 509, 78–87, https://doi.org/10.1016/j.epsl.2018.12.024, 2019.

Zhang, G., Luo, W., Chen, W., and Zheng, G.: A robust but variable lake expansion on the Tibetan Plateau, Sci. Bull., 64, 1306–1309, https://doi.org/10.1016/j.scib.2019.07.018, 2019.

Zhang, W., Wu, H., Cheng, J., Geng, J., Li, Q., Sun, Y., Yu, Y., Lu, H., and Guo, Z.: Holocene seasonal temperature evolution and spatial variability over the Northern Hemisphere landmass, Nat. Commun., 13, 5334, https://doi.org/10.1038/s41467-022-33107-0, 2022.

Zhao, B., Castaneda, I. S., Bradley, R. S., Salacup, J. M., de Wet, G. A., Daniels, W. C., and Schneider, T.: Development of an in situ branched GDGT calibration in Lake 578, southern Greenland, Org. Geochem., 152, 104168, https://doi.org/10.1016/j.orggeochem.2020.104168, 2021.

Zhao, C., Liu, Z. H., Rohling, E. J., Yu, Z. C., Liu, W. G., He, Y. X., Zhao, Y., and Chen, F. H.: Holocene temperature fluctuations in the northern Tibetan Plateau, Quat. Res., 80, 55–65, https://doi.org/10.1016/j.yqres.2013.05.001, 2013.

Zhao, C., Rohling, E. J., Liu, Z., Yang, X., Zhang, E., Cheng, J., Liu, Z., An, Z., Yang, X., Feng, X., Sun, X., Zhang, C., Yan, T., Long, H., Yan, H., Yu, Z., Liu, W., Yu, S.-Y., and Shen, J.: Possible obliquity-forced warmth in southern Asia during the last glacial stage, Sci. Bull., 66, 1136–1145, https://doi.org/10.1016/j.scib.2020.11.016, 2021.

Zheng, Y., Li, Q., Wang, Z., Naafs, B. D. A., Yu, X., and Pancost, R. D.: Peatland GDGT records of Holocene climatic and biogeochemical responses to the Asian Monsoon, Org. Geochem., 87, 86–95, https://doi.org/10.1016/j.orggeochem.2015.07.012, 2015.

Zhou, W., Yu, S.-Y., Burr, G. S., Kukla, G. J., Jull, A. J. T., Xian, F., Xiao, J., Colman, S. M., Yu, H., Liu, Z., and Kong, X.: Postglacial changes in the Asian summer monsoon system: a pollen record from the eastern margin of the Tibetan Plateau, Boreas, 39, 528–539, https://doi.org/10.1111/j.1502-3885.2010.00150.x, 2010.

Zielinski, G. A. and Mershon, G. R.: Paleoenvironmental implications of the insoluble microparticle record in the GISP2 (Greenland) ice core during the rapidly changing climate of the Pleistocene-Holocene transition, Geol. Soc. Am. Bull., 109, 547–559, https://doi.org/10.1130/0016-7606(1997)109<0547:piotim>2.3.co;2, 1997.